Characteristic of thermal energy system self-driven by exhausted heat from equipment in lunar base

Kai Zhang[a], Peijie Sun[b], Shuangfei Li[b], Catalina Spataru[c], Xiaojing Lv[*d], Yiwu Weng[*a],

[a] *School of Mechanical Engineering, Shanghai Jiao Tong University, Shanghai, 200240, China*

[b] *Aerospace System Engineering Shanghai, CASC, Shanghai, 201108, China*

[c] *Energy Institute, University College London, London, WC1H 0NN, UK*

[d] *China-UK Low Carbon College, Shanghai Jiao Tong University, Shanghai, 201306, China*

Abstract: The conditions on the moon surface swings between extreme heat and extreme cold. When receives full sunlight may reach temperatures of around 121℃, while when dark could drop to as low as -150 ℃. This makes difficult to coordinate and manage the heat inside the Lunar Base. In this paper, a novel topology of self-circulation thermal management system (STMS) is proposed, which can use the heat discharged from equipment module as system power to provide cooling capacity for manned module. Firstly, the internal and external thermal environment characteristics of Lunar Base are analyzed in this paper. Secondly, the thermodynamic model of the STMS is constructed to obtain the thermal performance of the STMS under the design condition and off-design conditions. Finally, typical working conditions of the STMS are analyzed. Results show that when Lunar Base is built in an area higher than 35 °N, the STMS can possess heat dissipation performance greater than 271W/m^2. Driven by 30kW heat discharged from equipment module, cooling capacity for manned module is enhanced by increasing evaporation temperature and refrigeration evaporation temperature or decreasing condensation temperature. The STMS can provide a maximum cooling capacity of 11.53kW and a minimum cooling capacity of 3.78KW for manned module. Above all, the STMS can operate independently without external power supply for 24 hours. This study provides insights on the technical operation of a Lunar Base in the future.

Key words: Thermal Management System; Thermal Self-circulation; Thermodynamics Analysis; Lunar Base

1. Introduction

The Moon is the closest celestial body to the Earth and is the base for humans to carry out deep space exploration [1,2]. The development and utilization of in-situ lunar resources attract countries to carry out continuous lunar exploration activities. The establishment of a "permanent Lunar Base" can carry out scientific activities in a low gravity environment, thus scientists could potentially explore the moon's lava tube caves, investigate hints of water ice found in the craters of the lunar poles, raising new research understandings. [3,4]. The advanced key technologies for exploring and developing lunar resources can not only be applied on earth, but also lay a technical foundation for future deep space exploration missions [5].

Several countries have successfully carried out a series of missions to the Moon [6]. Luna 2

* Co-Corresponding author: ywweng@sjtu.edu.cn (Yiwu Weng).

* Co-Corresponding author: lvxiaojing@sjtu.edu.cn (Xiaojing Lv).

was the first spacecraft to reach the surface of the Moon, and the first human-made object to contact another celestial body in 1959, which was the sixth of the Soviet Union's Luna program spacecraft launched to the Moon [7]. Apollo 15 was the ninth crewed mission in the United States' Apollo program and the fourth to land on the Moon, which was the first time that humans were successfully sent to the surface of the Moon (1969). Chinese Chang'e-5 successfully brought lunar samples back to earth in 2020 [8]. These milestones laid the interest in further exploration and the construction of a permanent Lunar Base.

As an indispensable part of establishing a "permanent Lunar Base", thermal management system (TMS) has been studied by scholars all over the world. In the 1990s, the Johnson Space Center (JSC) affiliated to NASA evaluated the performance of solar powered steam compression heat pump system based on two-phase fluid and put forward a heat management scheme of lunar permanent base based on heat pump [9]. The scheme considered that the steam compression heat pump powered by solar energy as the internal TMS of Lunar Base could improve the quality of the equipment heat and greatly enhance the effective heat emission capacity of the equipment. K. R. Sridhar et al. [10] used electromechanical heat pump to design and optimize the TMS suitable for Lunar Base, which could be used to discharge 100kW waste heat generated from Lunar Base. M. A. Lamber [11] conducted a comprehensive evaluation of the thermally driven adsorption heat pump system suitable for a permanent Lunar Base. Wenlian Ye et al. [12] proposed a heat dissipation method using heat pump to the problem that it is difficult to dissipate the heat inside Lunar Base due to the large-scale temperature change on the lunar surface at day and night. The results show that there was an optimal system quality and optimal heat dissipation temperature when equipment heat dissipation was certain. Dinghua Hu et al. [13] established a solar thermal storage power generation system based on the finite-time thermodynamics method to realize the in-situ utilization of lunar resources. The designed system could produce an average power of 6.5 kW during operation. At the nighttime, the utilization efficiency of solar energy collected during the daytime could reach 19.6%. Xiaochen Lu et al. [14] used finite-time thermodynamics to analyze the exergy of solar thermal power generation system in Lunar Base. Results show that there were different optimal temperatures of heat source under different ambient temperature and the optimal temperature of heat source decreased with the increase of ambient temperature.

In summary, scholars mostly use heat pump to dissipate the heat inside Lunar Base at present. However, heat pump system is driven by external power. During the long lunar nighttime, using heat pump system for dissipating heat will aggravate the problem of energy shortage. To find a new STMS suitable for Lunar Base, the previous research has been conducted under the funding of the China Manned Space Engineering Office. The previous research mainly focuses on feasibility study of different topologies of thermal management system and pursuing the working fluid with excellent cycle performance [15,16]. Based on the previous research, this paper analyzes the external thermal environment characteristics of Lunar Base to determine the scope of application of the STMS. The influence of key parameters, such as evaporation temperature (T_g), refrigeration evaporation temperature (T_e) and condensation temperature (T_c), deviating from the design condition on system performance is also considered in this paper. The changes of the external thermal environment of the Lunar Base and the astronauts' schedule will put forward different requirements for the STMS. Therefore, the performance of the STMS under typical working conditions is analyzed to verify whether the STMS can realize 24-hour self-circulation operation.

Fig. 1 shows a conceptual diagram of the STMS. This STMS is mainly combined with the

power cycle (PC) and the ejector refrigeration cycle (ERC). These two sub cycles are coupled with each other through the ejector and the radiator. In PC, the heat (Q_g) collected by cold plates usually comes from scientific research equipment (SRE), transportation equipment (TE), life assurance system (LAS), fuel cell power system (FCPS) and fire protection system (FPS), etc [17]. This heat can generate power (W_{power}) through the turbine. Most of the power (W_{re}) drives the ejector to provide cooling capacity (Q_e) for the manned module to ensure that astronauts and internal precision instruments work at normal temperature. In addition, excess power (W_{net}) can be supplied to the outside. Finally, the waste heat (Q_c) is dissipated into the deep space through the radiator. Furthermore, solar heat is used as auxiliary energy for the STMS during the lunar daytime. The STMS constructed in this paper includes the processes of heat collection, transmission, utilization and dissipation in Lunar Base. The STMS can be driven by the heat of the internal equipment module of Lunar Base to provide cooling capacity for the manned module and can realize self-circulating without external power supply.

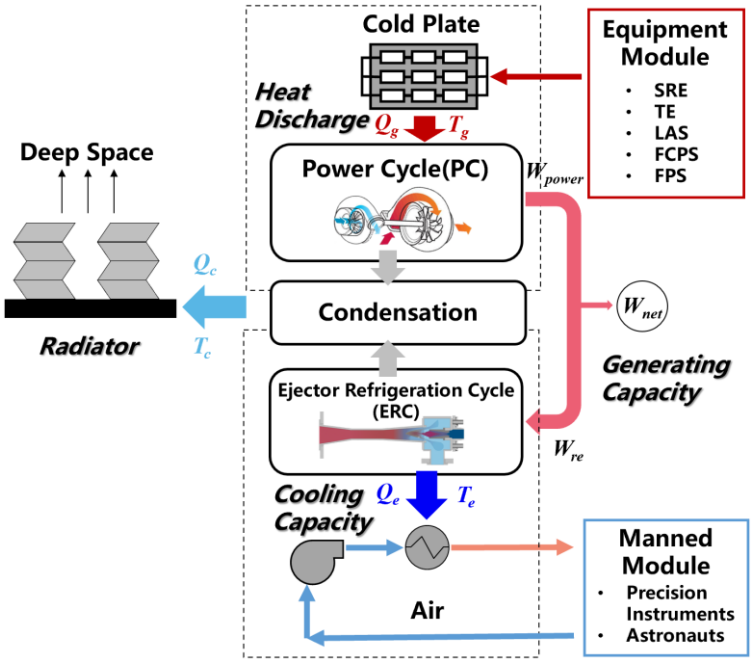

Fig. 1. Conceptual diagram of the STMS

2. Analysis of the STMS

Compared with the space station, Lunar Base has the characteristics of more cabin modules, more complex equipment, more variable grade and quantity of heat emission, which puts forward new requirements for STMS. The characteristic of external thermal environment and internal thermal environment of Lunar Base are analyzed in this section.

2.1. Heat dissipation capacity of the STMS

From the perspective of theoretical analysis, this section establishes the heat dissipation capacity model of STMS at the observation points on the lunar surface, based on Kepler's third law. The effect of the longitude and the latitude on the radiation intensity and surface temperature of Moon are analyzed subsequently. The space radiation heat flux received by the moon mainly comes from solar radiation, and a small part comes from earth radiation (less than 1%) [18]. Therefore, this paper mainly considers that the external space radiant heat flow of the system is solar radiation. Fig.

2 and Fig. 3 are the schematic diagram of the geometric relationship in the Sun-Earth-Moon system and the schematic diagram of the solar zenith angle on the lunar surface, respectively. According to Ref [19], the effective solar irradiance at any point on the lunar surface can be expressed by Eq. (1) to Eq. (4).

$$G_{eff} = G_{sun} \cdot \cos i = \frac{S_0 \sin^2\left(W_{em} R_{em} / R_{se}\right)}{R_{em}^2 \sin^2 W_{em}} \cos\left(A_i + B_i\right) \tag{1}$$

$$i = A_i + B_i \tag{2}$$

$$A_i = \arccos\left[-\sin W_q \sin W_p + \cos W_q \cos W_p \cos\left(J_q - J_p\right)\right] \tag{3}$$

$$B_i = \arcsin\left\{R_{moon} \sin A_i \Big/ \left[\frac{R_{em}^2 \sin^2 W_{em}}{\sin^2\left(W_{em} R_{em} / R_{se}\right)} + R_{moon}^2 - \frac{2 R_{em} R_{moon} \sin W_{em} \cos A_i}{\sin\left(W_{em} R_{em} / R_{se}\right)}\right]^{1/2}\right\} \tag{4}$$

Where, G_{Sun} is the solar irradiance in $W \cdot m^{-2}$. i is the solar zenith angle in degree. S_0 is the solar constant. W_{em} stands for the geocentric latitude of the Moon. R_{em} refers to the distance from the Earth to the Moon in AU. R_{se} is the distance from the Sun to the Earth in AU. P denotes the vertical incident point of sun light, and Q denotes the point of observation. J_p and J_q stand for the selenographic longitude of P and Q, respectively. W_p and W_q refer to the selenographic latitude of P and Q, respectively. R_{moon} is the radius of the moon in AU.

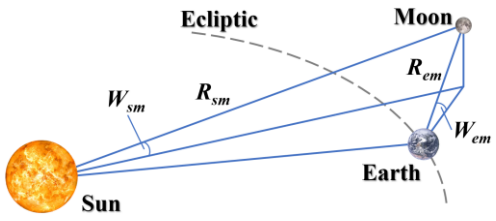

Fig. 2. The geometric relationship in the Sun-Earth-Moon system

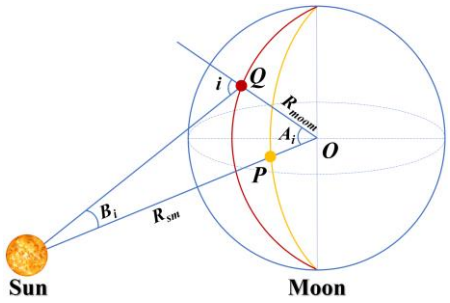

Fig. 3. The schematic diagram of the solar zenith angle on the lunar surface

The special thermal environment of Lunar Base brings great challenges to the heat dissipation of the STMS. The STMS can only dissipate heat into deep space through radiator. Different from heat dissipation of the space station using radiator, the radiator installed on the lunar surface will be affected by external radiation at any installation angle. Therefore, the research on the influence of radiator installation angle on heat dissipation capacity is the basis of subsequent performance research of the STMS. Three orientations are considered in this paper. They included (a) a vertical radiator perpendicular to the plane of the solar ecliptic, (b) a vertical radiator parallel to the plane of the ecliptic, and (c) a horizontal radiator insulated from the lunar surface (Fig 4) [20].

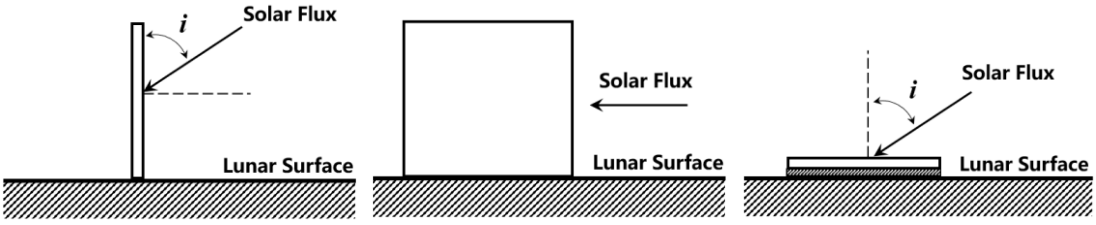

(a). a vertical radiator (b). a vertical radiator parallel (c). a horizontal radiator

perpendicular to the plane of the solar ecliptic | to the plane of the ecliptic | insulated from the lunar surface

Fig. 4. Radiator orientations

Different radiator orientations correspond to different sink temperatures (T_s), which can be calculated by the following equation [21].

Fig. 4(a)
$$T_s = \left(\frac{T_M^4}{2} + \left| \frac{G_{sun}\alpha_r}{2\sigma\varepsilon_r} \cos i \right| \right)^{1/4} \quad (5)$$

Fig. 4(b)
$$T_s = \frac{T_M}{1.189} \quad (6)$$

Fig. 4(c)
$$T_s = \left(\frac{G_{sun}\alpha_r}{\sigma\varepsilon_r} \cos i \right)^{1/4} \quad (7)$$

Where, T_M refers to the lunar surface temperature. α_r is the solar absorptance of the radiator. σ refers to the Stefan-Boltzmann constant, 5.67×10^{-8} W·m^{-2}·K^{-4}. ε_r stands for the emissivity coefficient of the radiator.

The surface temperature model of the Moon (T_M) is defined as below

$$T_M = \left[\frac{(1-\bar{A})}{\varepsilon} \frac{G_{eff}}{\sigma} + \frac{M}{\sigma} \right]^{1/4} \quad (8)$$

Where, $\bar{A}$ refers to the single-scattering albedo (approximately set to 0.127). ε represents the infrared surface emissivity of lunar surface (approximately set to 0.97). M is a subsurface cooling flux 6 W·m^{-2}.

According to different sink temperatures of different radiator orientations, corresponding heat dissipation capacity are calculated in a lunar month (Fig. 5-Fig. 7). Taking radiator orientations at Fig. 4(a) condition for example, the effects of longitude and latitude on heat dissipation capacity are shown in Fig. 5(a) and Fig. 5(b), respectively. It can be seen from Fig. 5(a), when the latitude is lower than 60 °N, the STMS loses its heat dissipation capacity, which is improved with increasing latitude. It can be concluded from Fig. 5(b) that longitude has no effect on peak heat dissipation capacity of STMS. Comparing Fig. 5 to Fig. 7, Fig.4(c) installation angles still have good heat dissipation capacity in low latitudes.

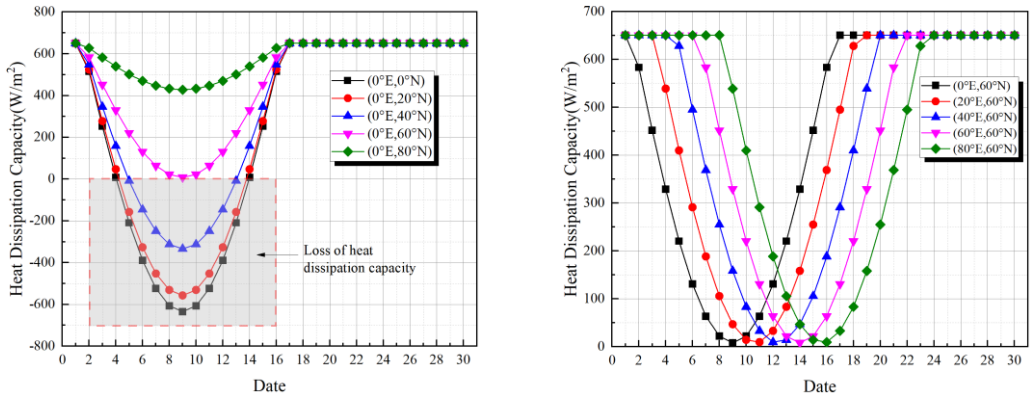

(a). At different latitudes (b). At different longitudes

Fig. 5. Heat dissipation capacity of Fig.4 (a) installation direction in a lunar month

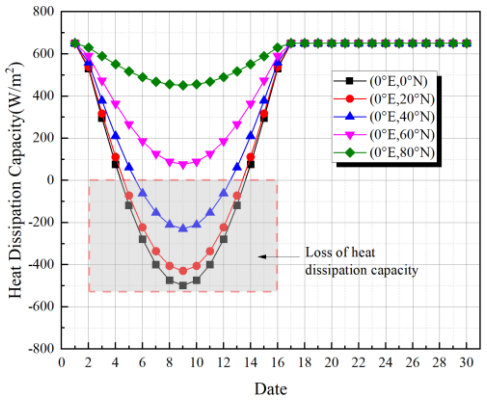

Fig. 6. Heat dissipation capacity of Fig.4 (b) installation direction in a lunar month

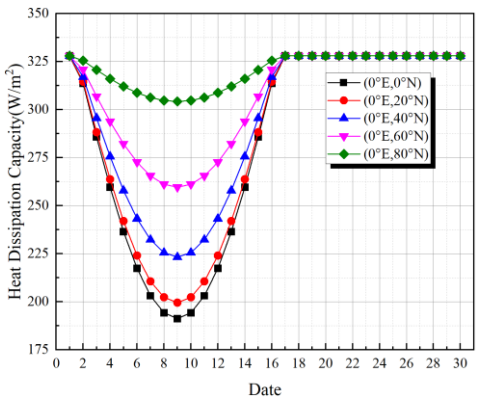

Fig. 7. Heat dissipation capacity of Fig.4 (c) installation direction in a lunar month

Fig. 8 presents the variation characteristics of the minimum heat dissipation capacity (G_{min}) of the radiator with three different installation angles under the same cold plate temperature during the daytime, when latitude changes form 0°N to 80°N. In Fig. 8, it is divided into three areas: I (0°N-35°N), II (35°N-71°N) and III (higher than 71°N). In the I(0°N-35°N) region, two kinds of radiators placed vertically even absorb heat due to high solar radiation at low latitude, and completely lose their dissipation capacity. In this area, the radiator placed horizontally can dissipate heat normally, but the heat dissipation capacity is poor, which is lower than the reference value of 217 W/m^2 of the International Space Station, which means that larger radiator area is required to dissipate the same quantity of heat, which undoubtedly improves the difficulty and cost of component transportation. In area II (35°N-71°N), two vertical radiant coolers still cannot work normally. On the contrary, in this latitude range, the radiator placed horizontally has better performance, and its heat dissipation capacity is higher than the reference value of 217 W/m^2 of the International Space Station. In the III (higher than 71°N) region, due to low solar irradiation, the radiator installed vertically has better performance than that placed horizontally. However, the low solar irradiance in this area will seriously affect the performance of photovoltaic array used in Lunar Base, so it is not recommended. In summary, the STMS with the radiator placed horizontally has better heat dissipation performance in the II (35°N-71°N) area, which can provide guarantee for the heat dissipation of the internal equipment of Lunar Base.

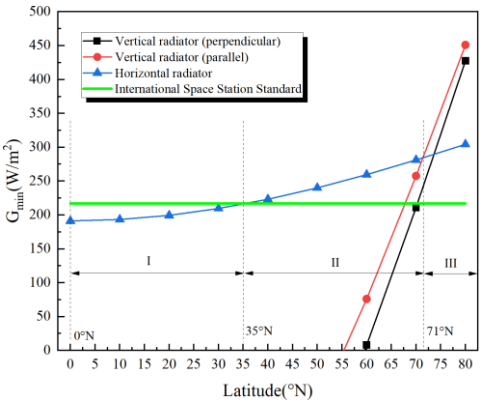

Fig. 8. Characteristics of G_{min} at different latitudes

2.2. Heat discharge and cooling demand in Lunar Base

In this section, the variation characteristics of system performance of equipment heat discharge and cooling capacity during a natural working day at nighttime are studied. The heat generated from the equipment module of Lunar Base considered in this paper mainly includes the heat discharged from SRE, TE, LAS, FCPS and FPS, etc. It should be noted that three subsystems are considered in LAS: SAWD (solid amine water desorbed), TIMES (thermoelectric integrated membrane evaporation system) and SPE (solid polymer electrolyte) systems. SAWD is used to remove carbon dioxide in manned module, TIMES uses membrane distillation to purify wastewater and urine, while SPE system obtains oxygen by electrolyzing water. Table 1 shows the power, temperature and dynamic characteristics of heating elements in the STMS loop [22].

Table 1 The power, temperature and dynamic characteristics of heating components

Components	Power (kW)	Temperature (℃)	Fluctuation Characteristics
SRE	15	40-60	Constant
FCPS	10	70-90	Constant
TE	2	50-70	Intermittent operation according to task
FPS	1.7	40-45	Constant
SAWD	1.5	30-40	Constant
TIMES	2.8	45-55	Four hours each day: 7:00 a.m.-9:00 a.m. 18:00 p.m.-20:00 p.m.
SPE	1.8	50-60	Constant

The cooling capacity is provided to astronauts and precision instruments in the manned module. The cooling capacity required by the precision instrument is 9kw when astronauts are working. Here, it is assumed that the cooling capacity of precision instruments required by astronauts at rest is only one third of that required by astronauts at work, i.e., 3KW. The cooling capacity of the astronauts is based on《HUMAN INTEGRATION DESIGN HANDBOOK (HIDH)》proposed by NASA [23]. Fig. 9 shows cooling capacity required at different astronaut activities during a standard mission day with exercise.

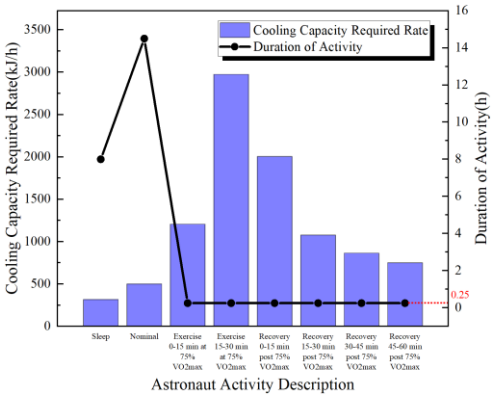

Fig. 9. Cooling capacity required at different astronaut activities

Based on the data in Fig. 9, it is assumed that the manned cabin contains 8 astronauts. Their schedule is considered as follow:

- Astronauts wake up at 7:00 a.m. and go to sleep at 23:00 p.m
- Two astronauts exercise four times as follow: 15:00-15:30, 15:30-16:00, 18:30-19:00 and 19:00-19:30. After each exercise time period, astronauts have one hour to recover.

According to the arrangement of the heating components and the astronauts' schedule, the heat discharge and cooling capacity characteristics of the STMS during a standard mission day can be obtained. Fig.10 shows the heat load from equipment module is maintained at about 30kW. When the TIMES subsystem starts to work, the heat load rises from 30kW to 32.8 kW. Compared with the heat load, the cooling capacity load fluctuates greatly. When the astronaut is sleeping, the cooling load required is 3.7kW. When the astronauts exercise, the maximum the cooling load required can reach 11.28kW. The characteristics of heat discharge and cooling capacity of the STMS during a standard mission day obtained in this section can provide data support for the calculation and analysis of subsequent typical working conditions.

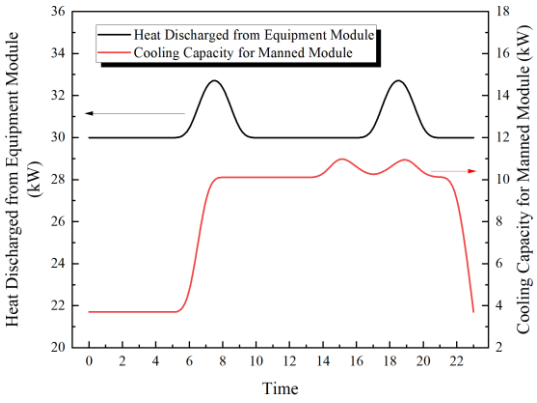

Fig.10. The characteristics of heat discharge and cooling capacity in a standard mission day

2.3. Composition and operation principle of the STMS

Fig. 11 shows a more specific topology model of the STMS. The main components of the STMS includes a pump, a turbine, an ejector, a cold plate (evaporator), a radiator, a refrigeration evaporator, an expansion valve, a solar collector (optional as auxiliary energy) and a generator.

The specific working process of the STMS is as follows: at point 1, the working fluid is pressurized by the pump and sent to the evaporator. The working fluid absorbs the heat discharged from the equipment module of Lunar Base in the evaporator, and changes from liquid to gas, thus completing the evaporation process. It should be noted that the superheated gaseous working fluid

can selectively absorb other high-temperature heat (solar energy or nuclear energy) during the daytime to further improve the evaporation temperature. Then, the superheated gaseous working fluid enters the turbine to expand and do work. The working fluid at turbine outlet (Point 8) is still in the overheated state and subsequently enters the ejector as the primary fluid. The primary fluid flows through the ejector nozzle and forms a low pressure at the nozzle outlet, to absorb the secondary fluid into the mixing chamber for mixing. The mixed fluid leaves the ejector through the diffuser. The working fluid at the outlet of the ejector subsequently enters the radiator to dissipate the heat to the deep space, and changes from gas to liquid to complete the condensation process. Part of the condensed liquid working fluid returns to the pump, and the other part enters the expansion valve. The pressure of working fluid is reduced by the expansion valve. Then, the working fluid enters the refrigeration evaporator to absorb the heat discharged from the manned module, changing from liquid to gas. The gaseous working fluid at the outlet of the refrigeration evaporator (Point 16) enters the ejector as a secondary fluid.

In the STMS, the turbine and the pump are coaxial, so the pump is driven directly by the turbine. Afterwards, the turbine drives ejector to provide cooing capacity for manned module. Excess power generated by the turbine can be transferred to the outside to realize independent thermal self-circulation operation of the STMS.

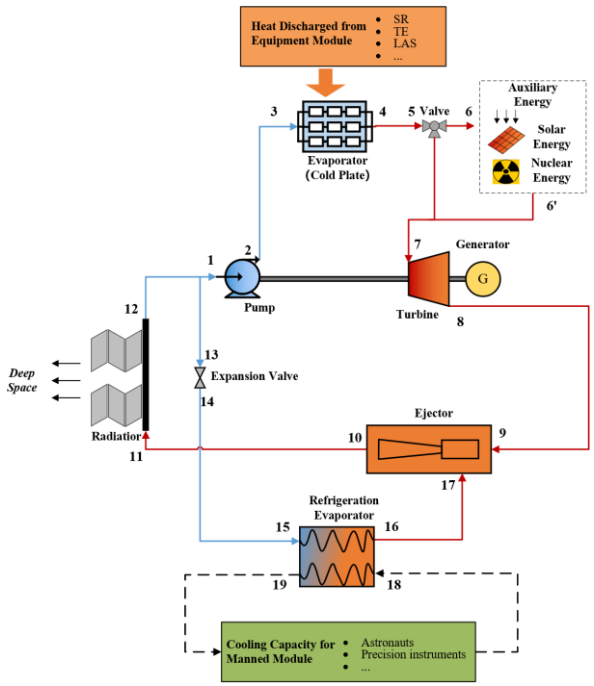

Fig. 11. Composition of the STMS

3. Theoretical model

Because the STMS is used in the Lunar Base environment, some requirements and assumptions need to be put forward to carry out the research. The requirements for state parameters of the STMS are as follows:

(1) The outlet temperature of the radiator is less than 20℃.

(2) The outlet temperature of the refrigeration evaporator is less than 20℃.

(3) R600a is selected as the system working fluid.

The following assumptions are made:

(1) It is assumed that the influence of gravity change is ignored on the performance of the component based on Refs. [24, 25, 26]. These references draw a conclusion that the influence of gravity on the two-phase heat transfer coefficient decreases with the increase of mass flow rate. Therefore, when building the component model, the working fluid is maintained in the state of high mass flow rate by adjusting the parameters to ignore the influence of gravity.

(2) Assuming that the shell of Lunar Base is well insulated from the external environment, the heat transfer between Lunar Base and the external environment only occurs in the radiator and the solar collector.

(3) It is assumed that the STMS is well insulated. Except for the evaporator and the refrigeration evaporator, other components have no heat exchange with the Lunar Base.

3.1. Pump model

The head and mass flow rate of the pump can be adjusted by changing the speed. According to the similarity law, the head and mass flow rate of the pump under off-design conditions can be obtained according to Eq. (9) and Eq. (10) [27].

$$\frac{H_{pump,off}}{H_{pump,d}} = \left(\frac{\omega_{pump,off}}{\omega_{pump,d}} \right)^2 \tag{9}$$

$$\frac{m_{pump,off}}{m_{pump,d}} = \frac{\omega_{pump,off}}{\omega_{pump,d}} \tag{10}$$

Where, $H_{pump,d}$ and $H_{pump,off}$ respectively represent the head at design condition and off-design condition, m. $\omega_{pump,d}$ and $\omega_{pump,off}$ respectively represent the speed at design condition and off- design condition, r/min. $m_{pump,d}$ and $m_{pump,off}$ respectively represent mass flow rate of the pump at design condition and off- design condition, kg/s.

The isentropic efficiency of the pump under off-design conditions can be calculated by equation (11).

$$\frac{1-\eta_{pump,off}}{1-\eta_{pump,d}} = \left(\frac{\omega_{pump,d}}{\omega_{pump,off}} \right)^{0.07} \tag{11}$$

Where, $\eta_{pump,d}$ and $\eta_{pump,off}$ respectively represent the isentropic efficiency of the pump at design condition and off-design condition.

The power consumption of the pump can be calculated by equation (12)

$$W_{pump} = m_{pump} \Delta h_{s,pump} / \eta_{pump} \tag{12}$$

Where, $\Delta h_{s,pump}$ is the isentropic enthalpy difference of the pump, kJ/kg.

3.2. Turbine model

The aerodynamic performance of the turbine under off-design conditions can be evaluated according to Stodola' ellipse method [28]. According to the turbine inlet conditions, the turbine constant φ can be obtained by equation (13).

$$\varphi = m_{tur} \frac{\sqrt{T_{tur,in}}}{P_{tur,in}} \tag{13}$$

The equations of turbine efficiency and outlet pressure under off-design conditions are given in Ref. [29]:

$$\eta_{tur,off} = \eta_{tur,d} \sin\left[0.5\pi \left(\frac{m_{tur,off}\rho_{tur,in,d}}{m_{tur,d}\rho_{tur,in,off}}\right)^{0.1}\right] \tag{14}$$

$$P_{tur,out,off} = \sqrt{P_{tur,in,off}^2 - m_{tur,off}^2 T_{tur,in,off} Y_d} \tag{15}$$

Where, $Y_d = \frac{P_{tur,in,d}^2 - P_{tur,out,d}^2}{P_{tur,in,d}^2 \varphi_d^2} \cdot \eta_{tur,d}$ and $\eta_{tur,off}$ respectively represent the isentropic efficiency of the turbine at design condition and off-design condition. $m_{tur,d}$ and $m_{tur,off}$ respectively represent mass flow rate of the turbine at design condition and off- design condition, kg/s. $\rho_{tur,in,d}$ and $\rho_{tur,in,off}$ respectively represent density at turbine inlet at design condition and off-design condition, kg/m^3. $P_{tur,in,off}$ and $P_{tur,out,off}$ respectively represent pressure at turbine inlet and outlet at off-design condition, Pa. $P_{tur,in,d}$ and $P_{tur,out,d}$ respectively represent pressure at turbine inlet and outlet at design condition, Pa. $T_{tur,in,off}$ represents temperature at turbine inlet at off-design condition, K.

The output power of the turbine can be calculated by Equation (16)

$$W_{tur} = m_{tur} \Delta h_{s,tur} / \eta_{tur} \tag{16}$$

Where, $\Delta h_{s,tur}$ is the isentropic enthalpy difference of the turbine, kJ/kg.

3.3. Ejector model

The ejector is the key equipment in the STMS, which plays two main roles in the system. Firstly, the ejector acts to compress the working fluid in the ERC. Secondly, the ejector can realize the mixing of the the working fluid at the outlet of the turbine and the outlet of the refrigeration evaporator. Fig. 12 shows the schematic of ejector, mainly composed of suction chamber, mixing chamber and diffuser. The ejector model in this study is based on theorem of momentum The mainly equations in the modeling process are summarized for easy reading in this paper [30,31, 32].

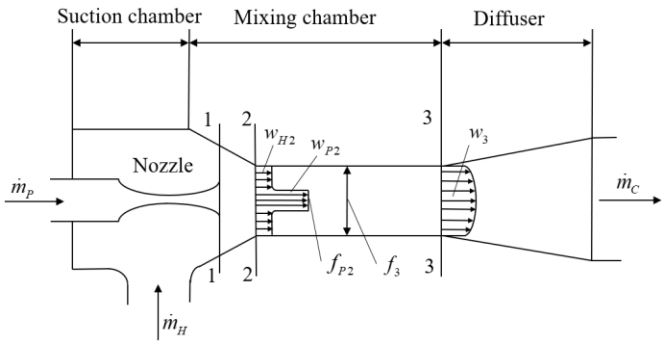

Fig. 12. Schematic of ejector

The momentum conservation equation is established between the section 2-2 of the throat inlet of the mixing chamber and the section 3-3 of the outlet of the mixing chamber as follows:

$$\varphi_2\left(\dot{m}_{\mathrm{P}} w_{\mathrm{P2}}+\dot{m}_{\mathrm{H}} w_{\mathrm{H2}}\right)-\left(\dot{m}_{\mathrm{H}}+\dot{m}_{\mathrm{P}}\right) w_3=\left(p_3-p_{\mathrm{P2}}\right) f_{\mathrm{P2}}+\left(p_3-p_{\mathrm{H2}}\right) f_{\mathrm{H2}} \tag{17}$$

Where, φ_2 stands for the coefficient of friction loss of mixing chamber. $\dot{m}$ is the mass flow rate of refrigerant. w refers to the velocity of refrigerant. p and f respectively represent the pressure and section area. The subscript "P", "H", "2" and "3" represent the primary fluid, the secondary fluid, the section of 2-2 and the section of 3-3 respectively.

The flow velocity of the primary fluid and the secondary fluid on the section 2-2, and the velocity of the mixed fluid on the section 3-3 of the mixing chamber outlet can be determined by Eq. (18), Eq. (19) and Eq. (20) respectively.

$$w_{\mathrm{P2}}=\varphi_1 a_{\mathrm{P}*} \lambda_{\mathrm{P2}} \tag{18}$$

$$w_{\mathrm{H2}}=\varphi_4 a_{\mathrm{H}*} \lambda_{\mathrm{H2}} \tag{19}$$

$$w_3=\frac{a_{\mathrm{c}*}}{\varphi_3} \lambda_{\mathrm{c3}} \tag{20}$$

Where, φ_1, φ_3 and φ_4 respectively stand for the coefficient of friction loss of nozzle, diffuser and suction chamber. $a_{\mathrm{P}*}$, $a_{\mathrm{H}*}$ and $a_{\mathrm{c}*}$ respectively represent the critical velocity of the primary fluid, the secondary fluid, and the mixed fluid. λ_{P2} and λ_{H2} respectively represent the velocity coefficients of the primary fluid and the secondary fluid on the 2-2 section, λ_{c3} is the velocity coefficients of the mixed fluid on the 3-3 section.

The entrainment ratio of ejector is determined by Eq. (21), based on the continuity equation and momentum conversion equation.

$$u\sqrt{\theta}=\frac{K_1 \lambda_{\mathrm{PH}}-K_3 \lambda_{\mathrm{c3}}}{K_4 \lambda_{\mathrm{c3}}-K_2 \lambda_{\mathrm{H2}}} \tag{21}$$

Where, u is the entrainment ratio, K_1~K_4 and θ can be calculated as the following equations:

$$K_1=\varphi_1 \varphi_2 \varphi_3 \tag{22}$$

$$K_2 = \varphi_2\varphi_3\varphi_4 \tag{23}$$

$$K_3 = 1+\varphi_3\frac{p_c}{p_p}\frac{\Pi_{c3}-\frac{p_H}{p_c}}{k\Pi_*\lambda_{c3}q_{PH}} \tag{24}$$

$$K_4 = 1+\varphi_3\frac{p_c}{p_H}\frac{\Pi_{c3}-\Pi_{c2}}{k\Pi_*\lambda_{c3}q_{H2}} \tag{25}$$

$$\theta = \frac{T_H}{T_P} = \frac{a_{H*}^2}{a_{P*}^2} \tag{26}$$

Where, λ_{PH} is equal to λ_{P2}, which denotes the velocity coefficients of the primary fluid on the 2-2 section. P_c is ejector outlet pressure. Π_{c2}, Π_{c3} and Π_* respectively indicate the relative pressure of 2-2 section, 3-3 section and the critical section. q_{PH} and q_{H2} respectively represent converted quality velocity of the primary fluid and the secondary fluid on the 2-2 section. k stands for the adiabatic exponent of refrigerant. T_P and T_H respectively mean the temperature of the primary fluid and the secondary fluid.

3.4. Radiator model

In this analysis, the radiator area is divided into three parts. The first part operates in the subcooled region which is denoted A_{rsc}. The second is the part operating in the two-phase region and is is denoted A_{rsat}. The third part operates in the superheated region and is denoted A_{rsh}. In the process of analysis, it is assumed that there is no temperature difference between the radiant cooling plate of the radiator and the working fluid at any given position. In this assumption, the thermal resistance of the receiver wall is ignored [33].

(1) Two-phase region analysis

$$A_{rsat} = \frac{\dot{m}[h_{sat}(x=1)-h_{sat}(x=0)]}{\varepsilon_r\sigma(T_{sat}^4-T_s^4)-G_{eff}\alpha_r} \tag{27}$$

Where, $\dot{m}$ is the mass flow rate coming into the radiator. $h_{sat}(x=1)$ stands for the dew point specific enthalpy. $h_{sat}(x=0)$ refers to the bubble point specific enthalpy. G_{eff} represents the effective solar irradiance. T_{sat} is the saturation temperature. T_s is the effective sink temperature.

(2) Superheated region analysis

$$A_{rsh} = \left\{\frac{2\tan^{-1}\left[\frac{b^{1/4}T^*}{a^{1/4}}\right]-\ln\left[a^{1/4}-b^{1/4}T^*\right]+\ln\left[a^{1/4}+b^{1/4}T^*\right]}{4b^{1/4}a^{3/4}}\right\}_{T_{in}^*}^{T_{sat}^*} \tag{28}$$

Where, $a = \frac{G_{eff}\alpha_r}{\dot{m}C_pT_c}+\frac{\varepsilon_r\sigma T_c^3}{\dot{m}C_p}T_s^4$, $b = \frac{\varepsilon_r\sigma T_c^3}{\dot{m}C_p}$, $T^* = \frac{T}{T_c}$. T_c refers to the condensation temperature. C_p stands for constant pressure specific heat capacity. $T_{sat}^* = \frac{T_{sat}}{T_c}\cdot T_{out}^* = \frac{T_{out}}{T_c}$. T_{out} refers to the radiator outlet

temperature.

(3) Subcooled region analysis

$$A_{rsc}=\left\{\frac{2\tan^{-1}\left[\frac{b^{1/4}T^{*}}{a^{1/4}}\right]-\ln\left[a^{1/4}-b^{1/4}T^{*}\right]+\ln\left[a^{1/4}+b^{1/4}T^{*}\right]}{4b^{1/4}a^{3/4}}\right\}_{T_{in}^{*}}^{T_{sat}^{*}} \tag{29}$$

Where, $T_{in}^{*}=\frac{T_{in}}{T_c}$. T_{in} refers to the radiator intlet temperature.

The total area of radiator (A_r) is equal to the sum of the areas of superheated zone, two-phase zone, and subcooled zone:

$$A_r=A_{rsat}+A_{rsh}+A_{rsc} \tag{30}$$

3.5. Solar collector model

During the daytime, the STMS can select solar energy as auxiliary energy to increase working fluid temperature [34,35]. Therefore, the model of solar collector is given in this section.

(1) Subcooled region analysis

$$A_{ssc}=\left\{\frac{2\tan^{-1}\left[\frac{b^{1/4}T^{*}}{a^{1/4}}\right]-\ln\left[a^{1/4}-b^{1/4}T^{*}\right]+\ln\left[a^{1/4}+b^{1/4}T^{*}\right]}{4b^{1/4}a^{3/4}}\right\}_{T_{in}^{*}}^{T_{sat}^{*}} \tag{31}$$

(2) Two-phase region analysis

$$A_{ssat}=\frac{\dot{m}[h_{sat}(x=1)-h_{sat}(x=0)]}{G_{eff}\alpha-\varepsilon\sigma(T_{sat}^{4}-T_{s}^{4})} \tag{32}$$

(3) Superheated region analysis

$$A_{ssh}=\left\{\frac{2\tan^{-1}\left[\frac{b^{1/4}T^{*}}{a^{1/4}}\right]-\ln\left[a^{1/4}-b^{1/4}T^{*}\right]+\ln\left[a^{1/4}+b^{1/4}T^{*}\right]}{4b^{1/4}a^{3/4}}\right\}_{T_{sat}^{*}}^{T_{out}^{*}} \tag{33}$$

Where, $a=\frac{G_{eff}\alpha_s}{\dot{m}C_pT_g}+\frac{\varepsilon_s\sigma T_g^{3}}{\dot{m}C_p}T_s^{4}$, $b=\frac{\varepsilon_s\sigma T_g^{3}}{\dot{m}C_p}$, $T^{*}=\frac{T}{T_c}$. T_g refers to the evaporation temperature, K. α_s is the solar absorptance of the solar collector. ε_s stands for the emissivity coefficient of the solar collector.

The total area of solar collector (A_s) is equal to the sum of the areas of superheated zone, two-phase zone and subcooled zone:

$$A_s=A_{ssat}+A_{ssh}+A_{ssc} \tag{34}$$

3.6. Expansion valve model

The state point 14 is the outlet state of the expansion valve, also the inlet state of the refrigeration evaporator. The pressure P_{14} at this point is the saturated evaporation pressure P_e corresponding to the refrigeration evaporation temperature T_e. The throttling process in the expansion valve is regarded as an isoenthalp process. The temperature T_{14}, entropy s_{14} and dryness x_{14} of state point 14 can be calculated from enthalpy h_{14} and pressure P_{14}.

$$P_{14} = P_e = P(T_e, x = 0) \tag{35}$$

$$h_{14} = h_{13} \tag{36}$$

$$T_{14} = T(P_{14}, h_{14}) \tag{37}$$

$$s_{14} = s(P_{14}, h_{14}) \tag{38}$$

$$x_{14} = x(P_{14}, h_{14}) \tag{39}$$

3.7. Performance parameters of the STMS

To determine the basic parameters of the system, it was assumed that system is in a steady state. The heat losses to the environment are negligible [36].

Operation cycle starts from point 1 (Fig.1). The power W_p is required for increasing the pressure from radiator $P_1$to evaporation P_2 level is equal to:

$$W_p = \dot{m}_{ORC} \cdot \eta_p \cdot \left(h_{2,isentropy} - h_1\right) \tag{40}$$

Where $\dot{m}_{ORC}$ is the mass flow rate in PC; η_p represents isentropic pump efficiency.

Next step in cycle is the evaporation process. Heat discharged from equipment module (Q_h) warms up the working fluid to change it from liquid to superheated steam. The heat flow transmitted can be calculated by Eq. (41).

$$Q_h = \dot{m}_{ORC} \cdot \left(h_3 - h_2\right) \tag{41}$$

The STMS can also absorb solar energy as auxiliary energy during the daytime to improve the energy grade of gaseous working fluid entering the turbine. Required heat fluxes are described as:

$$Q_{hs} = \dot{m}_{PC} \cdot \left(h_{6'} - h_6\right) \tag{42}$$

The superheated refrigerant expands in the turbine, in which the work is equal to:

$$W_t = \dot{m}_{PC} \cdot \eta_{tur} (h_{8,isentropy} - h_7) \tag{43}$$

Next step in cycle is the mixing process in ejector. The superheated refrigerant at the turbine outlet enters the ejector as a primary fluid which flows through the nozzle and accelerates within it. At the exit of the nozzle, the accelerated fluid becomes supersonic, which induces a locally low-pressure region at the exit of the nozzle. Hence, the vapor (the secondary fluid) from the refrigeration evaporator is sucked into the ejector. The primary and secondary fluids then mix in the mixing section and undergo a pressure recovery process in the diffuser section. Thermodynamic parameter of point 10 can be determined by point 9 and 17:

$$h_{10} = \left(h_9 + u \cdot h_{17}\right) / (1+u) \tag{44}$$

Where u is the entrainment ratio, $u = \dot{m}_{ERC} / \dot{m}_{ORC}$.

The combined fluid flows to the radiator where it condenses. The heat of condensation Q_c is rejected into the space environment. Q_c is given by:

$$Q_c = \left(\dot{m}_{ERC} + \dot{m}_{PC}\right) \cdot \left(h_{11} - h_{12}\right) \tag{45}$$

Where, $\dot{m}_{ERC}$ is the mass flow rate in ERC.

A part of the fluid at the outlet of the radiator flows into the pump to complete the PC, and another part of the fluid passes through the valve to complete the ejector refrigeration cycle. It is the isenthalpic process in the valve, so h_{14} equals to h_{13}.

Next step in cycle is the refrigeration evaporation process. Because of locally low-pressure region, the vapor from the refrigeration evaporator is sucked into the ejector as the secondary fluid. Therefore, heat discharged from manned module (Q_e) is absorbed by the evaporation process. Q_e is described as:

$$Q_e = \dot{m}_{ERC} \cdot \left(h_{16} - h_{15}\right) \tag{46}$$

Power generation efficiency is given by:

$$\eta = \frac{W_t}{Q_h + Q_{hs}} \tag{47}$$

Coefficient of Performance (COP) is described as:

$$COP = \frac{Q_e}{W_p + Q_{hs} + Q_h} \tag{48}$$

4. Characteristic analysis of the STMS

The STMS applied in Lunar Base has great difference between heat source and cooling source, where operation environment is different from the ground. Therefore, it is indispensable to select the optimal working fluid of the combined system. Because the small droplets generated by the condensation process can cause serious damage to the equipment, dry refrigerants are generally selected to prevent the condensation during the expansion process in the turbine and the ejector nozzle. According to the previous research, R600a is selected as working fluid in thermodynamic analysis. In this paper, system performance is calculated at the design condition and off-design conditions.

4.1. Characteristic of the STMS at design condition

Considering a variety of operating conditions, it is necessary to put forward requirements for each thermal state parameter and establish a design condition for comparison. Based on thermodynamic parameters under design conditions, when analyzing the impact of parameter changes on system cycle performance, only the corresponding parameters are changed, and the other parameters remain unchanged. Main design parameter requirements are shown in Table 2.

Table 2 Parameters at design condition

Parameter	Value	Unit
Heat discharged from equipment module (Q_h)	30	kW
Evaporation temperature (T_g)	315.15	K
Condensation temperature (T_c)	289.15	K
Refrigeration evaporation temperature (T_e)	286.15	K

Superheat at evaporator outlet (dT_g)	2	K
Subcooled temperature (dT_c)	2	K
Superheat at refrigeration evaporator outlet (dT_e)	2	K
Average radiation temperature of radiator (T_r)	283.15	K
Isentropic efficiency of pump (η_p)	0.75	/
Isentropic efficiency of turbine (η_t)	0.80	/
Efficiency of evaporator (η_e)	0.95	/
Efficiency of refrigeration evaporator (η_{re})	0.95	/
Resistance loss of heat exchangers (Δp_h)	6	%
Resistance loss of pipeline (Δp_p)	3	%

In the calculation, the heat discharge Q_h from the equipment module is 30 kW, the evaporation temperature T_g is 315.15k, the condensation temperature T_c is 289.15k, and the refrigeration evaporation temperature T_e is 286.15k. In engineering practice, the isentropic efficiency of turbine and pump is generally in the range of 0.5-0.9, so the isentropic efficiency of turbine and pump are selected as 0.80 and 0.75 respectively.

The calculation results are shown in Table 3. It can be seen form Table 3, when the STMS absorbs 30kW heat through cold plate, it can provide 10.26 kW cooling capacity for manned module meanwhile output 587.26 W power. At this design condition, entrainment ratio of ejector is equal to 0.38 and COP of the STMS can reach 0.34. Results show that performance of the STMS under the design condition meets the design requirements that the STMS absorbs the heat removal from the equipment module to provide cooling capacity for the manned module and can operate in self-circulating without additional external power supply.

Table 3 Cycle performance of the STMS under the design condition

Parameter	Value	Unit
Cooling capacity（Q_e）	10.26	kW
Condensation capacity（Q_c）	39.67	kW
Power consumption of pump（W_p）	65.69	W
Turbine output work（W_t）	652.95	W
Entrainment ratio of ejector（u）	0.38	/
COP	0.34	/
Mass flow rate in the PC（M_p）	78.76	g/s
Mass flow rate in the ERC（M_p）	29.93	g/s
Ejector compression ratio (P_c/P_h)	1.23	/
Ejector expansion ratio (P_p/P_h)	1.68	/

4.2. Characteristic of the STMS at off-design condition

(1) Effect of T_g on the STMS

Fig. 13 and Fig. 14 show COP, cooling capacity, entrainment ratio, mass flow and turbine expansion ratio of the STMS under different evaporation temperature. As can be seen from the figure, when T_g increases from 312.15k to 318.15K, Q_e increases from 2.99kw to 16.02kw, COP increases from 0.10 to 0.53, u increases from 0.11 to 0.60, and ER decreases from 1.39 to 1.24. On the premise of keeping the condensation temperature and refrigeration evaporation temperature of the STMS unchanged, with the increase of evaporation temperature, the first impact on turbine performance is caused. The increase of evaporation temperature increases the inlet pressure of the turbine. Because the mass flow of working fluid passing through the turbine changes little, the expansion ratio of the turbine finally decreases. Therefore, it can be concluded that the outlet pressure of the turbine increases with the increase of evaporation temperature. Higher primary fluid pressure of the ejector means stronger ability to entrain secondary fluid realizing higher entrainment ratio of ejector, which directly leads to the increase of mass flow in the refrigeration cycle. As a result, the cooling capacity provided by the refrigeration cycle of the thermal management system increases finally improving the refrigeration performance of the STMS.

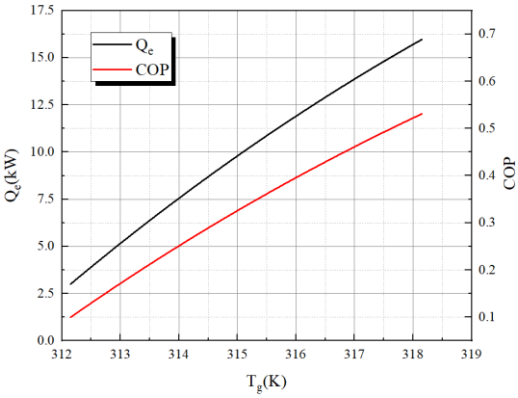

Fig. 13. COP and Q_e under different T_g

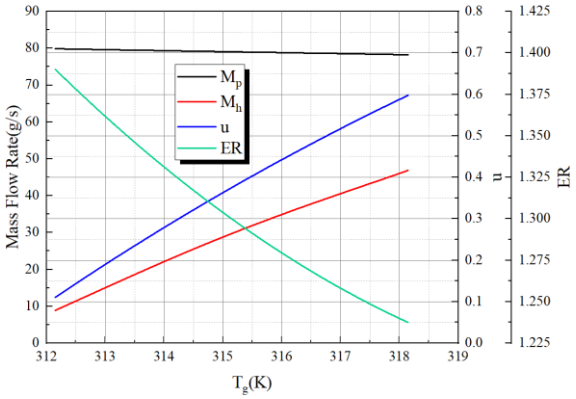

Fig. 14. M,u and ER under different T_g

(2) Effect of T_c on the STMS

Fig. 15 and Fig. 16 show COP, cooling capacity, entrainment ratio, mass flow and turbine expansion ratio of the STMS under different condensation temperature. As can be seen from the figure, when T_c increases from 288.55k to 289.15k, Q_e decreases from 12.4kw to 10.2kw, COP decreases from 0.41 to 0.33, u decreases from 0.46 to 0.38, and ER increases from 1.297 to 1.30. On the premise of keeping the evaporation temperature and refrigeration evaporation temperature of the STMS unchanged, increasing the condensation temperature can been seen that the primary fluid mass flow and turbine expansion ratio remain basically unchanged having little impact on the power cycle. The change of condensation temperature has a great impact on the performance of the ejector. The pressure at the outlet of the ejector is directly increased by increasing the condensation temperature. When the primary fluid pressure and secondary fluid pressure remain unchanged, entrainment ratio of ejector is decreased with increasing ejector outlet pressure. As a result, the cooling capacity provided by the refrigeration cycle of the STMS decreases, and finally leads to the reduction of the refrigeration performance.

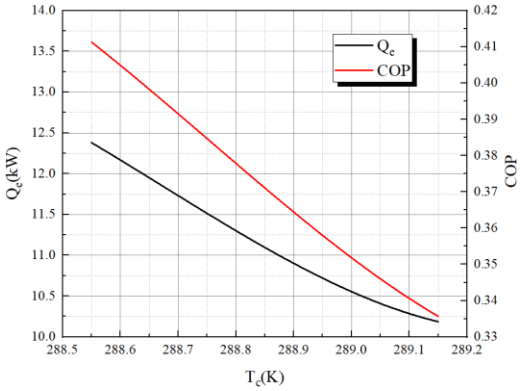

Fig. 15. COP and Q_e under different T_c

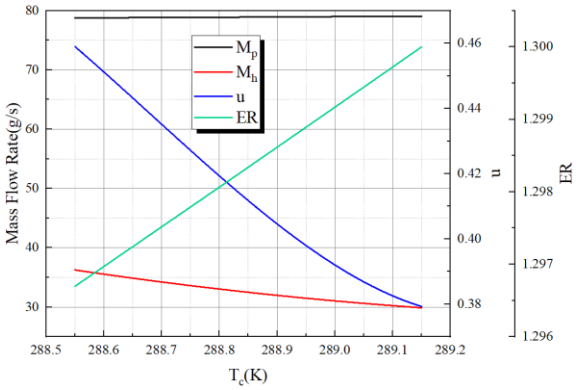

Fig. 16. M,u and ER under different T_c

(3) Effect of T_e on the STMS

Fig. 17 and Fig. 18 respectively show the COP, cooling capacity, entrainment ratio, mass flow and turbine expansion ratio of the STMS under different refrigeration evaporation temperature (T_e). It can be seen from the figure that when T_e increases from 286.15k to 286.75k, Q_e increases from 10.25kw to 11.36kw, COP increases from 0.34 to 0.38, u increases from 0.38 to 0.42, and ER basically remains unchanged at 1.3. On the premise of keeping the evaporation temperature and condensation temperature of the STMS unchanged, increasing the refrigeration evaporation temperature can see that it has little impact on the power cycle. The primary fluid mass flow and turbine expansion ratio remain basically unchanged. The change of refrigeration evaporation temperature has a great impact on the performance of the ejector. Increasing the refrigeration evaporation temperature directly increases the pressure at the secondary fluid inlet of the ejector. When the primary fluid pressure and the outlet pressure of the ejector remain unchanged, the increase of the primary fluid inlet pressure of the ejector will directly lead to the increase of the entrainment ratio, so as to increase the mass flow participating in the refrigeration cycle. As a result, the cooling capacity provided by the refrigeration cycle of the STMS increases, and finally leads to the improvement of the refrigeration performance.

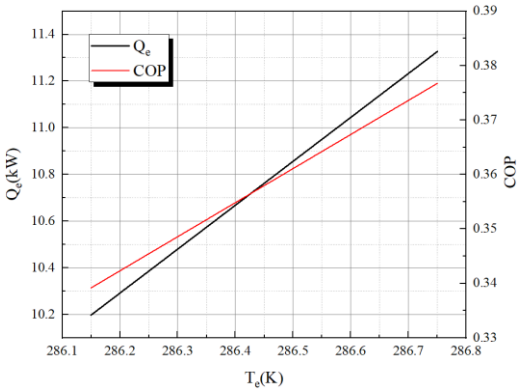

Fig. 17. COP and Q_e under different T_e

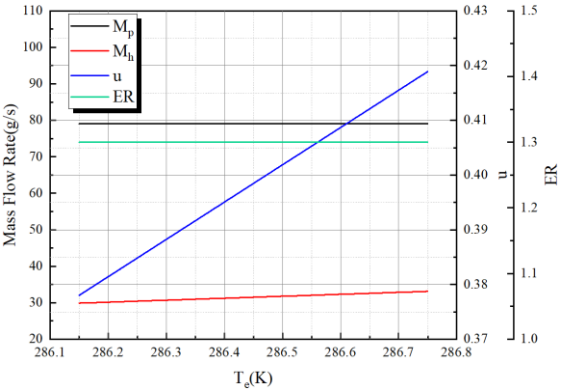

Fig. 18. M,u and ER under different T_e

4.3. Self-circulation characteristics of the STMS

Fig. 19 shows the characteristics of pump power consumption (W_p) and turbine output power (W_t). It can be found that W_p is maintained at about 66.7W at most times. When the astronauts are sleeping, the turbine output the maximum power, achieving 975.26W. However, when the astronauts are exercising, the turbine output the minimum power, achieving 744.99W. Results show that W_t is greater than W_p at any time. Fig. 20 shows the characteristics of cooling capacity (Q_e) and net output

power (W_{net}). It can be found that the STMS can provide a maximum power of 909.57W and a minimum power of 529.17W to the outside. A maximum and minimum Q_e of 11.53kW and 3.78KW are able to be provided for the manned cabin, respectively. It can be concluded from Fig. 19 and Fig. 20 that the STMS can realize self-circulation operation without the requirement of external power input and provide sufficient cooling capacity for the manned module.

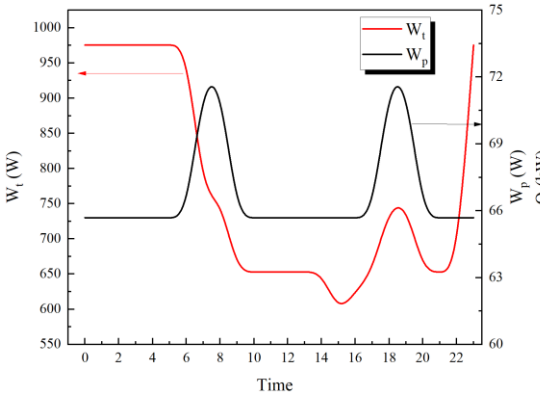

Fig. 19. Characteristics of W_p and W_t

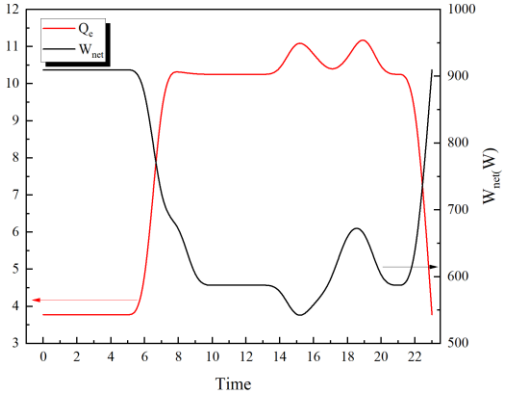

Fig. 20. Characteristics of Q_e and W_{net}

Fig. 21 shows the characteristics of COP and power generation efficiency (η). It can be found that when astronauts change from sleep to normal working state, COP increases from 0.13 to 0.34, while η decreases from 3% to 2%. The reason is that when astronauts start working normally, their metabolism will increase. At the same time, the precision instrument in the manned cabin is used more frequently so the cooling capacity required is strengthened. The increase of cooling demand means that the operation mode of the STMS should be switched from efficient power generation mode to high COP refrigeration mode by reducing turbine expansion ratio. On the premise that the turbine inlet temperature and pressure remain stable, reducing the turbine expansion ratio will increase the pressure of the primary fluid entering the ejector, resulting in higher primary fluid velocity at the nozzle outlet and lower pressure in the mixing chamber. The lower pressure in the mixing chamber means that the primary fluid with the same mass flow rate can suck more secondary fluid into the ejector for mixing.

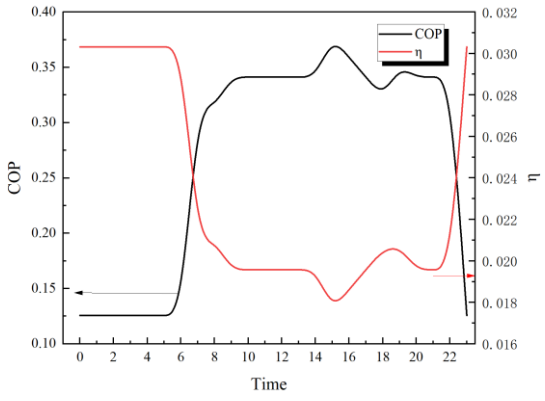

Fig. 21. Characteristics of COP and η

5. Analysis of typical working conditions of the STMS

Four working conditions for astronauts are considered: rest (I) and work (II) during nighttime, astronaut rest (III) and work (IV) during daytime. The system operation under these conditions is

calculated and analyzed.

5.1. Nighttime condition

(1) Astronauts rest (I)

Fig. 22 shows the key performance parameters under the rest conditions at nighttime. Under this condition, the cooling capacity of the system is 3.78kw, the COP is 0.13, the entrainment ratio of the ejector is 0.14, the turbine output work is 975.26w, and the pump power consumption is 65.69w. The system can not only discharge the heat from all equipment in the equipment module but also provide a cooling capacity of 3.78kw, which is greater than the cooling capacity demand of the manned module. In addition, the power generation of the system is much greater than that consumed by the pump, so it can also meet the needs of independent operation of the system. Therefore, the system can operate normally under this working condition and meet the needs of Lunar Base during the nighttime.

(2) Astronauts work (II)

Fig. 23 shows the key performance parameters under the work conditions at nighttime. The results show that the heat discharged from the equipment module is 32.8kw, the cooling capacity is 11.53kw, the COP is 0.35, the entrainment ratio of the ejector is 0.39, the turbine output work is 750.84w, and the pump power consumption is 71.82w. The system can discharge all the heat from the equipment and meet the cooling capacity demand of the manned cabin, and the turbine output power is much greater than the pump power consumption, so it can also meet the demand of independent operation of the system.

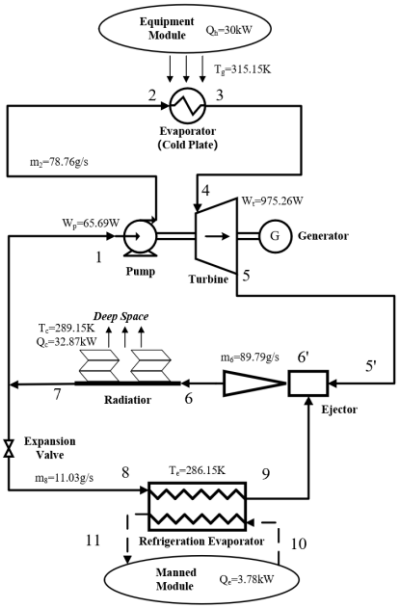

Fig. 22. Rest condition at nighttime

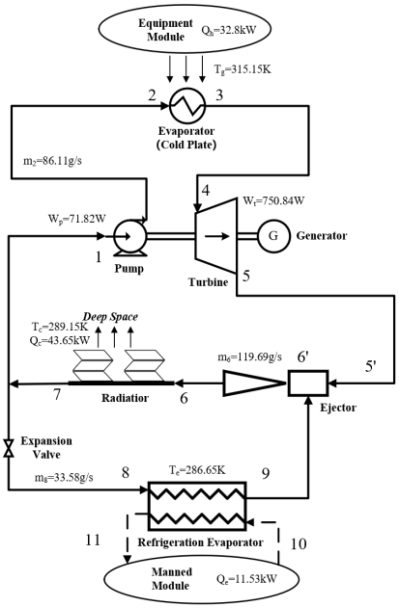

Fig. 23. Work condition at nighttime

5.2. Daytime condition

(1) Astronauts rest (III)

During the daytime, the external thermal environment of the STMS changes with the rotation of the moon, the effect of which is complex. When analyzing the performance of the STMS during the daytime, the value corresponding to the maximum effective solar irradiance is selected as the calculation condition, because if the thermal management system can effectively manage the heat of Lunar Base under this working condition, the designed STMS can also operate normally at other

working points. Under different working conditions of daytime and nighttime, the radiator has different heat dissipation capacity. Due to the irradiation of sunlight during the daytime, the heat dissipation performance of the radiator decreases, which leads to that the STMS requires larger effective radiation area than during the nighttime to take away as much heat as possible. The STMS is switched from nighttime to daytime mode, and the heat source in the power cycle has also changed. The system heat source includes not only the heat discharged from the equipment module, but also the heat discharged from the solar collector. Due to the higher thermal grade generated by solar energy, the evaporation temperature of the system can be improved, so that the working medium in the power cycle has more energy to drive the working fluid in the refrigeration cycle to realize the refrigeration of the manned module.

In the calculation, the peak effective solar irradiance at (0°E, 60°N) is taken as the reference value. Currently, the effective solar irradiance is 708.8 W/m^2. If the area of solar panel is 5m^2, the heat absorption of solar panel is 3.54kw. If the surface temperature of the radiator is equal to 10 ℃ and installed horizontally with an insulating layer separated from the lunar surface, it has a heat dissipation capacity of 259.66W/m^2.

Fig. 24 shows the key performance parameters under working conditions at nighttime. Under this condition, the performance parameters of the system are calculated. The results show that when the power cycle working fluid absorbs 30kW heat discharged from the equipment module and 3.54kw solar heat from solar collector, it can achieve a cooling capacity of 3.83kw, the COP is 0.11, the entrainment ratio of the ejector is 0.13, the turbine output work is 1.60kw, and the pump power consumption is 78.29w.

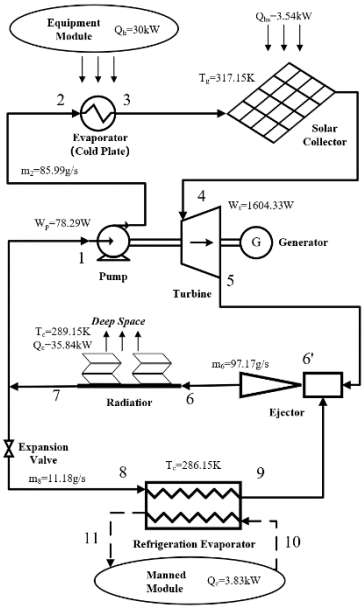

Fig. 24. Rest condition at daytime

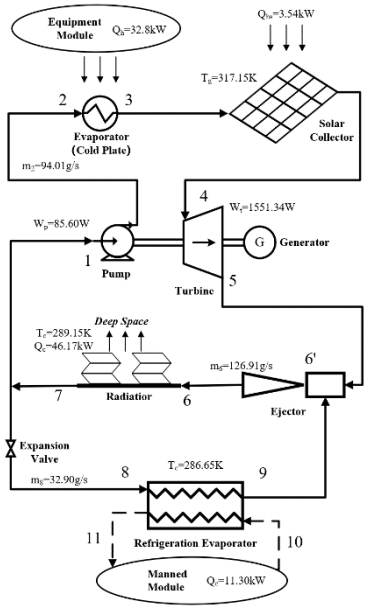

Fig. 25. Work condition at daytime

(2) Astronauts work (IV)

Fig. 25 shows the key performance parameters under work conditions at nighttime. Under this working condition, when the power cycle working fluid absorbs 32.8kw heat discharged from the equipment module and 3.54kW solar energy, it can achieve a cooling capacity of 11.30kw, the COP is 0.31, the entrainment ratio of the ejector is 0.35, the turbine output work is 1.55kw, and the pump power consumption is 85.60w. The system can discharge the heat from all equipment and meet the cooling capacity demand of manned module. In addition, the turbine power of the STMS is greater

than the pump power consumption, so it can also meet the requirements of independent operation of the system.

6. Conclusion

A novel thermal management system driven by the heat discharged from equipment module in Lunar Base has been proposed in this paper. A comprehensive study of internal and external thermal environment characteristic of the Lunar Base is carried out for the first time. The analysis results shows that the heat dissipation capacity of STMS is improved with increasing latitude. When the STMS is applied to the area higher than 35 °N, it has good heat dissipation performance (greater than 271W/ m^2), which can provide guarantee for the heat dissipation of equipment in Lunar Base.

At design condition, the STMS can provide 10.26 kW cooling capacity for manned module driven by 30kW heat discharged from equipment module. At off-design condition, cooling capacity provided by the STMS rises with increasing evaporation temperature and refrigeration evaporation temperature but decreases with increasing condensation temperature. Furthermore, self-circulation characteristics of the STMS is analyzed. The analyses show that the STMS can realize self-circulation operation without the requirement of external power input at any time of the day. The STMS can provide a maximum cooling capacity of 11.53kW and a minimum cooling capacity of 3.78KW to meets the cooling demand of the manned module.

Four extreme typical working conditions of Lunar Base are subsequently calculated and analyzed. Results show that when the astronauts start to rest from work at nighttime, the COP decreases by 63%. When the astronauts are at rest and the external thermal environment changes from nighttime to daytime, the turbine expansion ratio increases from 1.48 to 1.79, and the power generation efficiency increases from 3.03% to 4.55%.

The method of assessing the performance of the thermal management system used in Lunar Base proposed in this paper can provide technical support for the establishment of a permanent Lunar Base in the future. Additionally, current research focuses on the impact of internal and external thermal environment on thermal management system performance. In future work, influence of gravity variation on key processes, such as heat exchange process, expansion process and compression process, in the thermal management system will be analyzed. Besides, a semi-physical simulation platform needs to be established to verify the theoretical results.

Acknowledgements

The research is supported by the pre-research project of the China Manned Space Engineering Office under grant No. 17590501 and Shanghai Aerospace advanced technology joint research foundation under grant No. USCAST2019-6. The research is also supported by The National Natural Science Foundation of China under grant No. 52176014.

References

[1] Benaroya H. Lunar Habitats: A Brief Overview of Issues and Concepts." REACH 7-8. (2018): doi:10.1016/j.reach.2018.08.002.

[2] Crawford A, et al. Back to the Moon: The scientific rationale for resuming lunar surfa ce exploration. Planetary and Space Science 74.1(2012): doi:10.1016/j.pss.2012.06.002.

[3] Chavy-Macdonald MA, et al. The cis-lunar ecosystem — A systems model and scenari os of the resource industry and its impact. Acta Astronautica 188.(2021): doi:10.1016/J.AC

TAASTRO.2021.06.017.
[4] Palos MF, et al. Lunar ISRU energy storage and electricity generation. Acta Astronautica 170 (2020): doi:10.1016/j.actaastro.2020.02.005.
[5] Heinicke C, Arnhof M.A review of existing analog habitats and lessons for future lunar and Martian habitats. REACH (2021): doi:10.1016/J.REACH.2021.100038.
[6] Bonneville R. A truly international lunar base as the next logical step for human spaceflight. Advances in Space Research 61.12(2018): doi:10.1016/j.asr.2018.03.035.
[7] Slyuta E. Sample Return Missions: CHAPTER 3 - The Luna program (2021): doi:10.1016/B978-0-12-818330-4.00003-3.
[8] Zhou C, et al. Scientific objectives and payloads of the lunar sample return mission—Chang'E-5. Advances in Space Research (2021): doi:10.1016/j.asr.2021.09.001.
[9] Hanford A, Ewert M. An Assessment of Advanced Thermal Control System Technologies for Future Human Space Flight. SAE International (1996): doi:10.4271/961480.
[10] Sridhar KR. Thermal control systems for low-temperature heat rejection on a lunar base. NASA-CR-190063,1992:1-35.
[11] Lambert MA. Comparison of Heat Pumps for Permanent Lunar Base. Journal of Thermophysics and Heat Transfer: doi:10.2514/1.21683.
[12] Ye W, etc. Performance Analysis of Heat Rejection System for Lunar Base Heat Pump. Vacuum & Cryogenics (2015): doi:10.3969/j.issn.1006-7086.2015.04.011.
[13] Hu D, et al. A solar thermal storage power generation system based on lunar in-situ resources utilization: modeling and analysis. Energy 223.(2021): doi:10.1016/J.ENERGY.2021.120083.
[14] Lu X, et al. Exergy analysis of a lunar based solar thermal power system with finite-time thermodynamics. Energy Procedia 158.(2019): doi:10.1016/j.egypro.2019.01.209.
[15] Sun PJ, etc. Self-circulating heat management and power generation system for lunar base. Chinese Patent, No. 109612132, 2020.
[16] Chi L. Simulation Research on Thermal Management System of Lunar Base. Shanghai Jiao Tong University, Master Degree; 2021.
[17] Wang JX, et al. A highly self-adaptive cold plate for the single-phase mechanically pumped fluid loop for spacecraft thermal management. Energy Conversion and Management 111.(2016): doi:10.1016/j.enconman.2015.12.051.
[18] Yutian S, et al. Effects of solar radiation, terrestrial radiation and lunar interior heat flow on surface temperature at the nearside of the Moon: Based on numerical calculation and data analysis. Advances in Space Research 60.5(2017): doi:10.1016/j.asr.2017.05.013.
[19] Xuan F, Qiang G. The lunar surface temperature real-time model. Journal of Remote Sensing (2017): doi:10.11834/jrs.20177353.
[20] Simonsen, LC, Debarro MJ, Fa.Rmer JT. Conceptual design of a lunar base thermal control system. 1992.
[21] Dallas T, Diaguila AJ, Saltsman JF. Design studies on the effects of orientation, lunation, and location on the performance of lunar radiators.1971.
[22] Xianghua X. Numerical and Experimental Simulations of Dynamic Thermal Management of Small Scale Space Station. Tsinghua University, PhD; 2003.
[23] Allen C, etc. HUMAN INTEGRATION DESIGN HANDBOOK (HIDH). NASA, 2014.
[24] Ohta H. Experiments on microgravity boiling heat transfer by using transparent heater

s. Nuclear Engineering and Design 175.1(1997): doi:10.1016/S0029-5493(97)00172-6.
[25] Siegel R. Effects of Reduced Gravity on Heat Transfer. Advances in Heat Transfer (1967): doi:10.1016/S0065-2717(08)70274-0
[26] Lee H, et al. Experimental and theoretical investigation of annular flow condensation in microgravity. International Journal of Heat and Mass Transfer 61.(2013): doi:10.1016/j.ijheatmasstransfer.2013.02.010.
[27] Fan G, et al. Off-design behavior investigation of the combined supercritical CO2 and organic Rankine cycle. Energy 237.(2021): doi:10.1016/J.ENERGY.2021.121529.
[28] Cooke DH. On Prediction of Off-Design Multistage Turbine Pressures by Stodola's Ellipse. Journal of Engineering for Gas Turbines and Power 107.3(1985): doi:10.1115/1.3239778.
[29] Gabbrielli R. A novel design approach for small scale low enthalpy binary geothermal power plants. Energy Conversion and Management 64.(2012): doi:10.1016/j.enconman.2012.04.017.
[30] Zhen B, Weng Y. Theoretical and experimental study on a combined For Low Power and Ejector Refrigeration Cycle Temperature Heat sources. Shanghai Jiao Tong University, PhD; 2010.
[31] Zheng B, Weng Y W. A combined power and ejector refrigeration cycle for low temperature heat sources[J]. Solar Energy, 2010, 84(5): 784-791.
[32] Wang, JX, et al. A gas-atomized spray cooling system integrated with an ejector loop: Ejector modeling and thermal performance analysis. Energy Conversion and Management 180.(2019): doi:10.1016/j.enconman.2018.10.095.
[33] Kandil SM, Analysis and Optimization of a Jet-pumped Combined Power/Refrigeration Cycle. University of Florida, PhD; 2006.
[34] Yu HS, et al. Optimal design and operation of an Organic Rankine Cycle (ORC) system driven by solar energy with sensible thermal energy storage. Energy Conversion and Management 244.(2021): doi:10.1016/J.ENCONMAN.2021.114494.
[35] Serale G, et al. Formulation of a model predictive control algorithm to enhance the performance of a latent heat solar thermal system. Energy Conversion and Management 173.(2018): doi:10.1016/j.enconman.2018.07.099.
[36] Guilherme S, et al. Analytical model for thermal efficiency of organic Rankine cycles, considering superheating, heat recovery, pump and expander efficiencies. Energy Conversion and Management 246.(2021): doi:10.1016/J.ENCONMAN.2021.114628.